

See discussions, stats, and author profiles for this publication at: <https://www.researchgate.net/publication/231394322>

Theoretical Investigation of the Structure and Spectra of Zinc Phthalocyanines

ARTICLE *in* THE JOURNAL OF PHYSICAL CHEMISTRY · FEBRUARY 1995

Impact Factor: 2.78 · DOI: 10.1021/j100007a023

CITATIONS

22

READS

9

2 AUTHORS, INCLUDING:



[John O. Morley](#)

Swansea University

113 PUBLICATIONS 1,681 CITATIONS

SEE PROFILE

Theoretical Investigation of the Structure and Spectra of Zinc Phthalocyanines

John O. Morley*

Chemistry Department, University College of Swansea, Singleton Park, Swansea, SA2 8PP, U.K.

Michael H. Charlton

Research Centre, Zeneca Specialties, Hexagon House, Blackley, Manchester, M9 3DA, U.K.

Received: September 23, 1994[®]

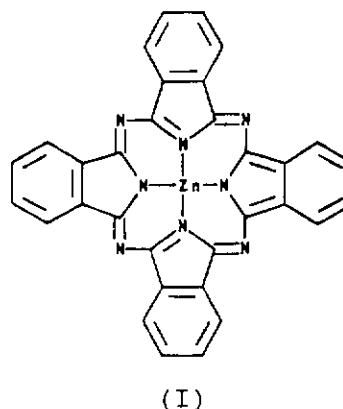
Calculations are reported on the structure, transition energies, and oscillator strengths of zinc phthalocyanine using a combination of the AM1 method and a version of the CNDO/S method, respectively. The origin of the experimental Q- and B-absorption bands has been explored in terms of the electronic transitions between occupied and virtual orbitals. The change in position of the electron densities in the frontier HOMO and LUMO molecular orbitals has been used to rationalize the effect of substituents on the experimental absorption maximum. Electron donors in the phenyl rings facilitate electron transfer from the HOMO to the LUMO and result in large bathochromic shifts.

Introduction

The phthalocyanines or tetraazatetraphenylporphyrins (I) have attracted considerable attention since their discovery and characterization in the first half of this century,^{1,2} and the copper derivative is a well-established commercial pigment. The bivalent metallic derivatives have D_{4h} symmetry and show very strong absorptions in the visible and near ultraviolet region with a strong Q-band at around 660 nm and a weaker B-band at around 330 nm (Table 1). Both bands are doubly degenerate in most metal complexes, though in metal-free phthalocyanine they are split because of the change to D_{2h} symmetry.

Theoretically, the spectroscopic properties of the phthalocyanines have been calculated using a number of different molecular orbital approaches.^{1,2} For example, the π -electron PPP method³ gives reasonable correlations between theory and experiment for transition energies of the Q-band and B-bands using a limited configuration interaction treatment level and a geometry based on the X-ray coordinates of nickel phthalocyanine.^{4,5} The spectroscopic properties of both zinc phthalocyanine⁶ and copper phthalocyanine⁷ have been calculated using a similar approach but with the inclusion of valence electrons at copper to predict metal-related transitions.⁷ The valence electron CNDO/S method⁸ has been applied to the study of the dianions of phthalocyanine using an extensive configuration interaction treatment⁹ and with a geometry based on crystallographic data from iron phthalocyanine. The calculated results show a good correlation with the spectra obtained for the zinc and magnesium complexes and suggest that the presence of the metal ion influences the oscillator strengths of the major transitions more strongly than it influences the transition energies.⁹ More recently, the INDO/S¹⁰ method has been used to calculate the spectra of nickel phthalocyanine¹¹ using a geometry based on crystallographic data.

Although there is a considerable body of experimental data available on the effect of substituents on the spectra of phthalocyanines (Table 1), there have been few theoretical attempts to rationalize this data. A recent study explores the effects of both electron attractors and donors on the spectra of the closely related free base porphyrins using both X-ray photoelectron spectroscopy and ab initio self consistent field



calculations, and a good correlation is reported between theory and experiment for a number of derivatives even though a fixed geometry is used for the macrocyclic ring.¹²

The present studies have been carried out to theoretically explore and interpret the effect of substituents on the spectra of substituted phthalocyanines. Unlike previous studies, we have optimized the structures of all the derivatives and then calculated their transition energies and oscillator strengths.

Methods of Calculation

The semiempirical AM1 method¹³ of the MOPAC package¹⁴ was used to calculate the structures of all the phthalocyanines described here. The resulting structures were then used as input for the spectroscopic calculation. In the CNDOVS method adopted,¹⁵ the off-diagonal elements of the core Hamiltonian are modified by the use of the CNDO/S spectroscopic constant, K , which distinguishes between the σ - and π -orbitals⁸ so that

$$H^{\sigma} = \frac{1}{2}(\beta_A + \beta_B)S_{ik}$$

$$H^{\pi} = \frac{1}{2}K(\beta_A + \beta_B)S_{ik}$$

where β_A and β_B are empirical bonding parameters and S_{ik} is the overlap integral between orbitals ϕ_i at atom A and ϕ_k at atom B. Furthermore, the monocentric bielectronic repulsion integrals, Γ_{AA} , are made a function of shell and orbital type with

[®] Abstract published in *Advance ACS Abstracts*, January 1, 1995.

TABLE 1: Effect of Substitution on the Absorption Maxima and Extinction Coefficients (in Parentheses) of Tetra- and Octasubstituted Metal Phthalocyanines (I)

metal		substituent	positions	Q-band	B-band	solvent ^a	ref
Zn	a	none		661	327	VAP ^b	19
	a	none		672	346	DMSO	19
	b	OPh	(α) 1,8,15,22	694 (5.31)	318 (4.63)	MCB	20
	c	OPh	(β) 2,9,16,23	681 (5.08)	326 (4.79)	MCB	20
	d	SPh	(α) 1,8,15,22	715 (5.17)	337 (4.63)	TCB	20
	e	SPh	(β) 2,9,16,23	692 (5.24)	351 (4.72)	TCB	20
	f	OMe	(α) 1,8,15,22	707	340	MCB	21
	g	OMe	(β) 2,9,16,23	680	346	MCB	21
	h	NMe ₂	(α , 1,8,15,22,- β) 3,10,17,24	786 (5.03)	340 (4.83)	MCB	22
	i	'Bu CN	(β , 2,3,9,10, β) 16,17,23,24	687 658	348 325	DMF VAP ^b	23 19
Cu	j	none		671	327	DMSO	19
	j	none		799		H ₂ SO ₄	23
	k	NMe ₂	(α) 1,8,15,22	778		DMF	22
	l	NMe ₂	(β) 2,9,16,23	730		DMF	22
	m	NMe ₂	(α , 1,8,15,22,- β) 3,10,17,24	782 (5.08)	336 (4.89)	MCB	22
	n	NH ₂ 'Bu	(α , 1,8,15,22,- β) 3,10,17,24	770 (5.25)	331 (4.69)	MCB	22
	o	NMe ₂	(α , 1,2,8,9,15, β) 16,22,23	708		DMF	22
	p	SO ₂ NMe ₂	1, 8,15,22	662	340	DMF	24
	q	SO ₂ NMe ₂	2, 9,16,23	671	341	DMF	24
	r	SO ₂ NMe ₂	1, 3,8,10, 15, 17,22,24	677	348	DMF	24
	s	CO ₂ H	(β , 2,3,9,10, β) 16,17,23,24	690	348	DMF	23
	t	CN	(β , 2,3,9,10, β) 16,17,23,24	686	349	DMF	23
	t	CN	2, 3,9,10, 16, 17,23,24	742		H ₂ SO ₄	23
	u	Cl	(α) 1,8,15,22	690		CLN	25
	v	Cl	(β) 2,9,16,23	679		CLN	25
	w	Cl	(α , 1,4,8,11, α) 15,18,22,25	705		CLN	25
	x	NO ₂ 'Bu	(α , 1,8,15,22,- β) 3,10,17,24	679 (5.13)	350 (4.70)	MCB	26

^a DMSO = dimethyl sulfoxide; MCB = chlorobenzene; TCB = trichlorobenzene; DMF = dimethylformamide; PYR = pyridine; THP = tetrahydrofuran/pyridine; CLN = chloronaphthalene. ^b Vapor phase spectrum recorded between 550 and 600 °C.

$$\Gamma_{AA} = C\langle\phi_i^2(1)|r_{12}^{-1}|\phi_j^2(2)\rangle$$

$$\text{where } C = [C_i(n,1)C_j(n,1)]^{-1/2}$$

and n is the principal quantum number, l is the azimuthal quantum number (orbital), and C_i and C_j are core coefficients for atomic orbitals ϕ_i and ϕ_j centered at atom A.¹⁶ The value of K was adjusted to 0.75 with $C = 0.33$ as in previous studies.¹⁵ The adjusted values of the monocentric integrals are also reflected in the two-center terms, Γ_{AB} , using the approximation¹⁷

$$\Gamma_{AB} = e^2/[r_{AB} + 2e^2/(\Gamma_{AA} + \Gamma_{BB})]$$

The initial wave function is expanded in terms of a configuration interaction treatment involving the 64 lowest energy transitions between the occupied and virtual orbitals (ϕ) in terms of the expansion coefficients, A , to give refined excited state wave functions, ϕ_n , defined as¹⁸

$$\phi_n = \sum A_{n,i-j}|\phi_i - \phi_j\rangle$$

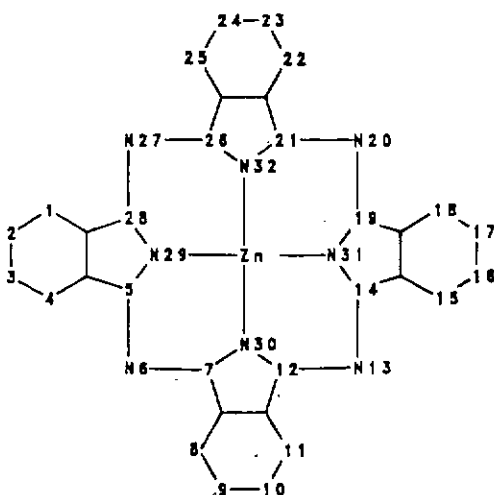
Although there is a considerable body of experimental data available showing the effect of substitution on a number of metal phthalocyanines such as the copper and zinc derivatives¹⁹⁻²⁶ (Table 1), calculations were carried out on zinc phthalocyanine as a representative member of the phthalocyanines because (1)

AM1 parameters are available for zinc²⁷ and (2) the closed shell electronic configuration $3d^{10}4s^2$ for zinc is easier to calculate spectroscopically than an open shell system.

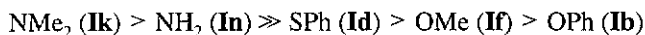
Attempts to calculate zinc phthalocyanine using parameters for zinc derived previously by one of us for the ground state properties of zinc chelates²⁸ gave an erroneous ordering of the low energy occupied orbitals with a σ -molecular orbital containing contributions from the zinc d_{x-y} atomic orbital inserted between the HOMO and HOMO-1. Both the bonding parameters, β_A , and the Mulliken electronegativities, E_n , where $E_n = -1/2(I + A)$ and I and A are the orbital ionization potentials and electron affinities, respectively, of the CNDOVS method were adjusted systematically until the correct orbital order was obtained. This involved raising the energy of the zinc $3d$ -orbitals and lowering the energy of the bonding interactions to give selected values (in electronvolts of $\beta_{Zn}(4s) = \beta_{Zn}(4p) = -15.0$, $\beta_{Zn}(3d) = -1.0$; $E_n(4s) = 4.08$, $E_n(4p) = 1.16$; and $E_n(3d) = 16.5$. Furthermore, because the bonding parameter adopted for chlorine in the CNDO/S method⁸ does not generally reproduce the electron-attracting character of the element in conjugated systems of the type described here, the value of $\beta_{Cl}(3p)$ was adjusted from the literature value of -15 to -30 eV.

Discussion

1. Experimental Spectra of Substituted Phthalocyanines. The effect of substitution on the spectra of the phthalocyanines has been reported for a number of metals as well as for the

SCHEME 1: Substituent Numbering Convention Used for Zinc Phthalocyanine

metal-free system, and the shifts observed for the zinc and copper derivatives (**Ia–Ii** and **Ij–Ix**)^{19–26} are comparable with the metal showing little effect (Table 1). The presence of electron donors in each of the four benzene rings (see Scheme 1 for the key to substitution positions) produces a bathochromic shift with the greatest effect found for substitution at the α -ring positions with the order



Of the donor effects reported, the symmetrical α -tetrakis-(dimethylamino)phthalocyanines (**Ih**, **Ik**, and **Im**) show shifts of more than 100 nm relative to the unsubstituted derivatives (**Ia** and **Ij**), though the effect of the same substituents at the β -ring positions (**Il**) is only roughly half this value.²² However, the presence of two adjacent dimethylamino groups at the α - and β -positions of each benzene ring to give an octasubstituted phthalocyanine (**Io**) results in a much smaller shift²² probably because the conjugation with the ring is reduced by steric clash between the methyl groups. Although the tetrathiophenoxyphthalocyanines (**Id** and **Ie**)²⁰ show a smaller shift than the corresponding amines (**Ik** and **Il**), the hexadecasubstituted derivative is almost colorless with its main Q-absorption band in the infrared region.²⁹

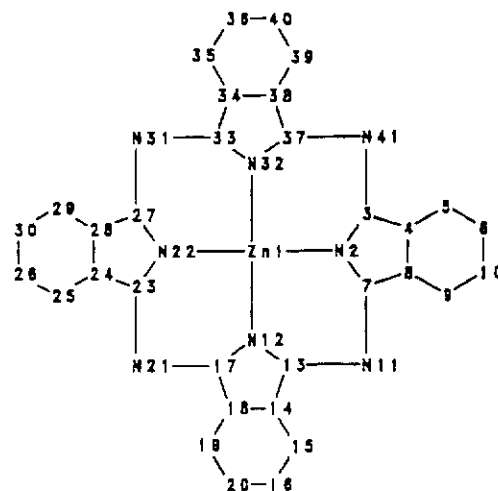
The effect of electron attractors on the spectra of the phthalocyanines, however, is considerably less pronounced, with surprising small bathochromic shifts observed (Table 1). Although the very small shift observed for the α -tetranitrophthalocyanine (**Ix**)²⁶ may be explained by a nonplanar conformation for the nitro group arising from the interaction of one oxygen atom with the lone pair of electrons at the nitrogen ring of the large ring (see later), the octacyano derivatives (**Ii** and **It**),²³ which show a similar small shift, are almost certainly planar. A similar small bathochromic effect is produced by the sulphonamido group (**Ip**, **Iq**, and **Ir**),²⁴ by the carboxyl group (**Is**),²³ and by chlorine (**Iu**, **Iv**, and **Iw**).²⁵ However, the complete substitution of all hydrogen atoms by fluorine to give either the copper or zinc hexadecafluorophthalocyanine produces little effect, and the materials resemble the hydrocarbon analogues.³⁰ Although electron attractors in the benzene rings produce a relatively small effect, protonation at the peripheral ring nitrogen atoms, using sulfuric acid, produces very large shifts, as shown for the copper derivatives (**Ij** and **It**).

2. Molecular Structures. Although there are crystallographic data available for a number of phthalocyanines,³¹ the molecules are not symmetric because the D_{4h} symmetry of the

TABLE 2: Comparison of Average Experimental and Calculated Structures for Zinc Phthalocyanine (I)

parameter ^a	I ^b	I ^c
Zn ₁ –N ₂	1.979	2.029
N ₂ –C ₃	1.369	1.398
C ₃ –C ₄	1.450	1.488
C ₄ –C ₅	1.393	1.384
C ₅ –C ₆	1.394	1.401
C ₄ –C ₈	1.401	1.433
C ₆ –C ₁₀	1.397	1.396
C ₇ –N ₁₁	1.331	1.350
Zn ₁ –N ₂ –C ₃	125.43	124.75
N ₂ –C ₃ –C ₄	108.89	107.85
C ₃ –C ₄ –C ₅	132.00	132.34
C ₄ –C ₅ –C ₆	117.20	118.00
C ₅ –C ₄ –C ₈	106.53	106.90
C ₅ –C ₆ –C ₁₀	121.29	121.24
N ₁₁ –C ₇ –N ₂	127.79	128.84
C ₁₃ –N ₁₁ –C ₇	123.48	122.84

^a Bond lengths in angstroms, angles in degrees. ^b X-ray data from the Cambridge Structural Database (CSD Refcode PTHCZN).³¹ ^c Calculated AM1 structure using *z*-matrix input with full symmetry constraints.

SCHEME 2: Numbering Convention Used for the AM1 Structure Optimization of Zinc Phthalocyanine

molecule is perturbed by crystal-packing forces. Attempts to optimize guessed structures for zinc phthalocyanine based on Cartesian coordinates from crystallographic data always produced a slightly unsymmetrical result (a known deficiency of the AM1 method^{13,14}) which did not give the known doubly degenerate excited states for the Q- and B-bands on subsequent CNDOVS spectroscopic calculation. This result did not improve with the adoption of more precise convergence criteria. For this reason, the structure optimization was carried out using a *z*-matrix input with symmetry constraints,¹⁴ but even here the calculation was fraught with difficulty and only succeeded when a specific atom-labeling procedure was adopted (see Scheme 2).

The results obtained show an excellent correlation between the calculated angles and the average experimental angles derived from crystallographic data (Table 2). The calculated bond lengths, however, are generally overestimated, though within 3% of the experimental data. Because the effect of substitution on the ring structure is largely unknown, all the structures discussed here were fully optimized using the *z*-matrix procedure with symmetry constraints.

3. Spectroscopic Calculations on Zinc Phthalocyanine. The symmetrical AM1-optimized structure for zinc phthalocyanine (**I**) was used directly for calculation of the transition energies, oscillator strengths, and orbital analysis using the

TABLE 3: Calculated versus Experimental Spectra for Zinc Phthalocyanine (Ia)^a

band	theory		experimental data			
	λ	f^b	vapor ^b		solution ^c	
	λ	f^b	λ	A	λ	ϵ
Q	685	1.18	661	1.3	678	200 000
B	295	2.11	327	1.0	349	57 500

^a λ is the transition energy, f is the oscillator strength, and ϵ is the extinction coefficient. ^b Data from ref 19, where A is the approximate ratio of the area under the absorption bands. ^c Data from ref 32 for the soluble tetra(*tert*-butyl) derivative in benzene.

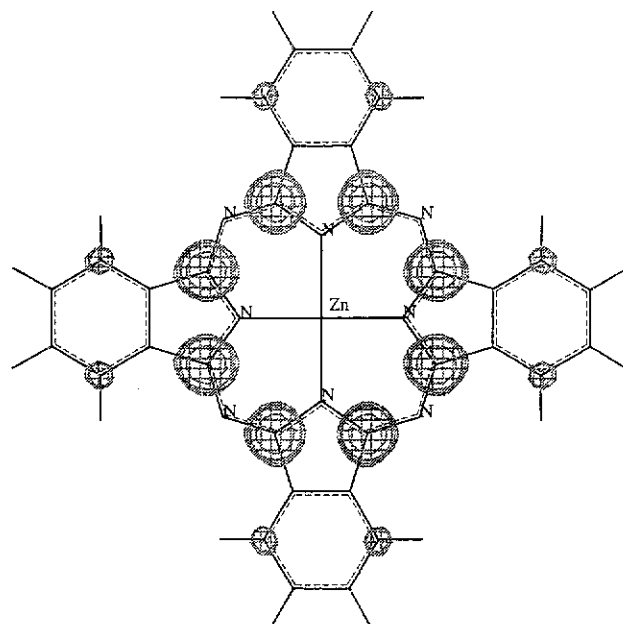
modified CNDOVS program,¹⁵ and the results were then compared with experimental data (Table 3).

3.1. Transition Energies and Oscillator Strengths. The calculated transition energy for the Q-band of zinc phthalocyanine (Ia) shows an excellent correlation with the experimental data derived from both vapor phase and solution measurements, though the transition energy of the B-band is somewhat overestimated. In addition, the oscillator strength of the Q-band appears to be underestimated (or conversely, the B-band overestimated) by comparison with the experimental extinction coefficients, which show that the former is around 3–4 times stronger than the latter. However, because the oscillator strength is more closely related to the integrated area under the absorption band rather than the extinction coefficient itself (which is the band height), an analysis of the approximate area under each of the absorption bands using data from ref 19 shows a better fit with the experimental data (Table 3).

3.2. Orbital Analysis. Both the Q- and B- bands arise from π -electron transitions from occupied to unoccupied orbitals. At the CNDOVS level of approximation in the ground state, there are a total of 196 valence electrons accommodated in the first 98 orbitals. An analysis of the orbital contributions after configuration interaction (Table 4) shows the low-energy Q-band is mainly composed of π -electron transitions from the HOMO (ϕ_{98}), with a much smaller contribution from the HOMO-1 (ϕ_{97}), to the two degenerate LUMOs (ϕ_{99} and ϕ_{100}).

In contrast, the higher energy B-band is dominated by transitions from the HOMO-1 (ϕ_{97}) to the two degenerate LUMOs (ϕ_{99} and ϕ_{100}), though in this case there are a number of other smaller contributions from other transitions (Table 4). Because the transitions are dominated by a relatively small number of occupied and unoccupied molecular orbitals, an increase in the number of configurations has little effect on either the composition of the excited state wave function or the transition energies. Thus, an increase in the number of configurations from 50 to 100 results in only a 4.5 nm change in the transition energy for the Q-band and a smaller effect on the B-band.

The large oscillator strengths obtained for these transitions (Table 3) reflect large changes in the electron distribution on

**Figure 1.** Position and magnitude of the electron density in the HOMO (ϕ_{98}) of zinc phthalocyanine.

excitation. The composition of the participating molecular orbitals (in terms of the molecular position of the wave function) and the orbital energies are found to be similar for both the CNDOVS and AM1 methods (Scheme 3).

A plot of the square of the wave function at the AM1 level using the Sybyl molecular modeling program³³ shows that the electron density of the HOMO is located mainly over the heterocyclic ring carbons at the 5-, 7-, 12-, 14-, 19-, 21-, 26-, and 28-positions, with smaller but significant contributions over the phenyl ring carbons at the 1-, 4-, 8-, 11-, 15-, 18-, 22-, and 25-positions (Figure 1). This distribution changes dramatically when an electron is excited into either LUMO (ϕ_{99} or ϕ_{100}), however, with the electron density now distributed over the eight nitrogen atoms, with a little remaining in the phenyl rings concentrated at the 2-, 3-, 9-, 10-, 16-, 17-, 22-, and 25-positions (Figure 2).

These results suggest that the presence of electron attractors at the peripheral ring nitrogens would stabilize the LUMO by pulling the electrons from the α -positions of the phenyl rings at the 1-, 4-, 8-, 11-, 15-, 18-, 22-, and 25-positions and thus facilitate the electron excitation process (Scheme 4a). However, a more powerful effect would be expected from the presence of donors in the phenyl rings since they are able to effectively transfer electrons specifically to both the four peripheral nitrogens at the 6-, 13-, 20-, and 27-positions and the four ring nitrogens at the 29-, 30-, 31-, and 32-positions by the classical mechanism illustrated (Scheme 4b,c). Although this effect

TABLE 4: Composition of the Key Excited States of Zinc Phthalocyanine (I) after Configuration Interaction

N^a	band	excited state	λ^b	composition ^c
50	Q	1	685.4	$-0.155\phi_{97-100} - 0.965\phi_{98-99} + 0.204\phi_{98-100}$
		2	685.4	$0.155\phi_{97-99} - 0.204\phi_{98-99} - 0.965\phi_{98-100}$
	B	12	295.3	$-0.215\phi_{97-99} + 0.891\phi_{97-100} - 0.157\phi_{98-99}$
		13	295.3	$-0.176\phi_{87-100} - 0.108\phi_{93-100} - 0.274\phi_{98-107}$
100	Q			$0.891\phi_{97-99} + 0.215\phi_{97-100} + 0.157\phi_{98-100}$
				$-0.176\phi_{87-99} + 0.108\phi_{93-99} + 0.274\phi_{98-108}$
				$-0.158\phi_{97-100} - 0.978\phi_{98-99} + 0.112\phi_{98-100}$
				$0.158\phi_{97-99} - 0.112\phi_{98-99} - 0.978\phi_{98-100}$
	B	15	295.8	$-0.390\phi_{97-99} - 0.799\phi_{97-100} + 0.140\phi_{98-99} +$
				$0.192\phi_{87-100} + 0.207\phi_{93-100} - 0.222\phi_{98-107}$
		16	295.8	$0.799\phi_{97-99} + 0.390\phi_{97-100} + 0.140\phi_{98-100}$
				$-0.192\phi_{87-99} + 0.207\phi_{93-99} + 0.222\phi_{98-108}$

^a Number of configurations. ^b Transition energy (in nm). ^c Major contributions greater than 0.1 are shown.

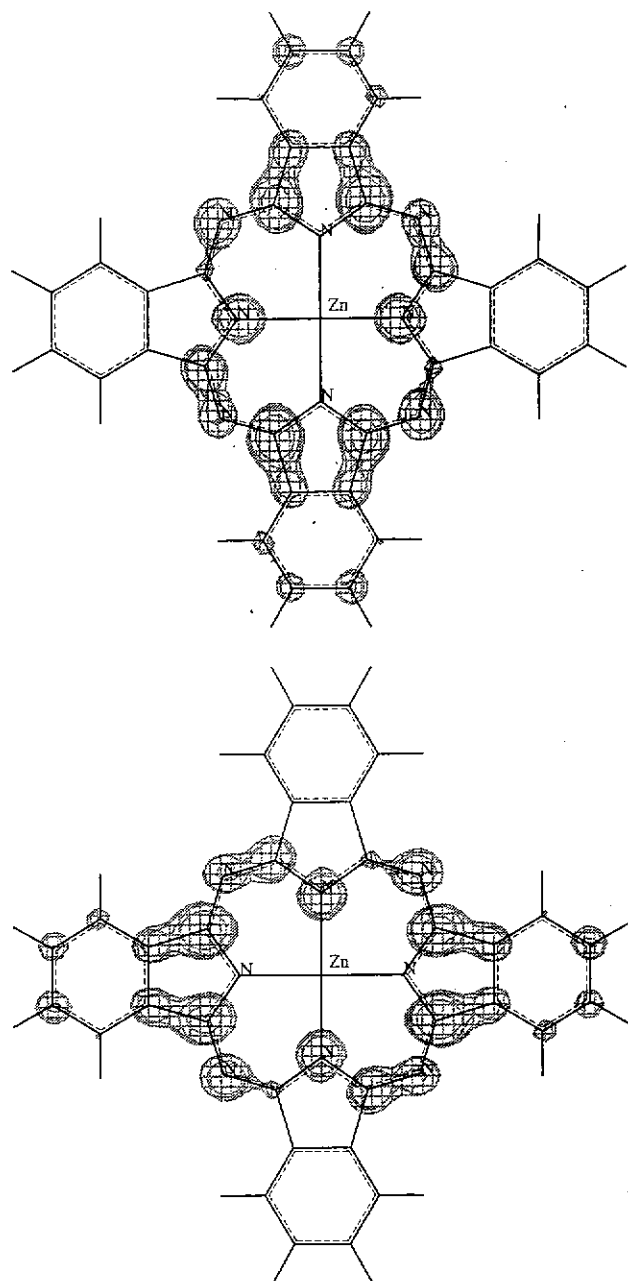





Figure 2. Position and magnitude of the electron density in the LUMOs of zinc phthalocyanine (ϕ_{99} , top, and ϕ_{100} , bottom).

SCHEME 3: Relative π -Orbital Energies (eV) in Zinc Phthalocyanine Calculated before CI Using the CNDOVS and AM1 Methods

		CNDOVS	AM1
LUMO	doubly degenerate 	+3.38	+4.47
HOMO			
HOMO-1		-2.63	-2.50

applies to donors at both the α - and β -positions of the phenyl rings, the former are likely to show a larger effect than the latter because some electron density is transferred to the β -positions of the phenyl rings in the transition from the HOMO to the LUMO (Figure 2). Both types of substituent, therefore, are likely to give rise to a lower energy transition from HOMO to LUMO, in line with experimental data obtained either from protonation at the four peripheral nitrogens or from the insertion

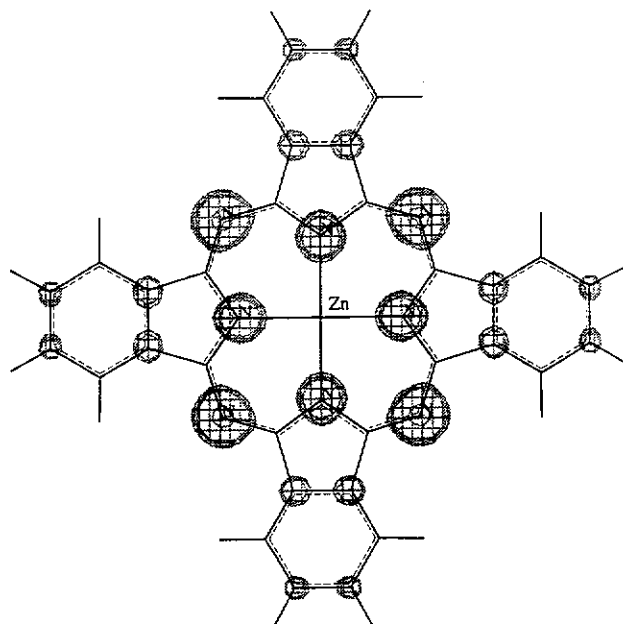
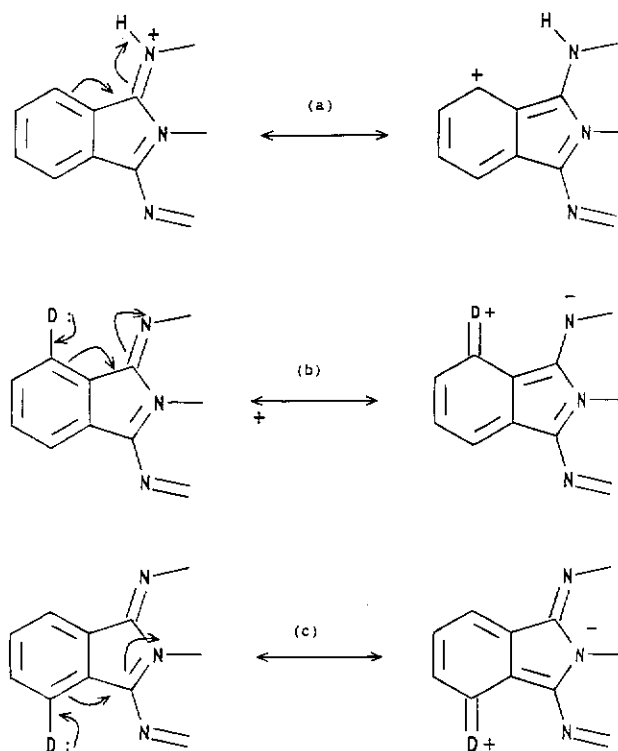


Figure 3. Position and magnitude of the electron density in the HOMO-1 (ϕ_{97}) of zinc phthalocyanine.

SCHEME 4: Stabilization of the LUMO of Zinc Phthalocyanine by the Presence of Either Electron Attractors at the Peri Positions (a) or Donors at the Phenyl Rings (b and c).



of four powerful electron-donating N,N -dimethylamino groups into the phenyl rings (Table 1).

The B-band of zinc phthalocyanine is dominated by the transition from the HOMO-1 to the two degenerate LUMOs. The electron density found in the HOMO-1 is located mainly at the eight nitrogen atoms (Figure 3). In each LUMO substantial electron density remains distributed over the peripheral nitrogens at the 6-, 13-, 20-, and 27-positions, but part is transferred from the four ring nitrogens at the 29-, 30-, 31-, and 32-positions to the carbons of the five-membered heterocyclic rings and a smaller amount to the phenyl rings (Figure 3). Neither the presence of donors nor attractors in the phenyl

TABLE 5: Effect of Substitution on the Calculated Transition Energies and Oscillator Strengths of Substituted Zinc Phthalocyanine (I) Optimized at the AM1 Level^a

no.	substituents and position ^b		heat of formation ^c	Q-band			B-band	
	α	β		λ	f	λ^d	λ	f
none			372.2	685	1.18	672	295	2.11
4	OH		207.6	722	1.30		297	1.66
4	OMe		233.4	717	1.28	707	299	1.56
4	SMe		385.0	705	1.24		293	1.95
4	NH ₂		360.6	743	1.32	770 ^e	292	0.90
4		NH ₂	367.5	712	1.20		288	0.40
4	NHMe		380.5	743	1.31		292	1.06
4	NMe ₂		447.6	757	1.30	778	296	0.71
4	NMe ₂ ^f		423.5	700	1.23	778	295	1.94
4		NMe ₂	408.7	721	1.21	730	288	0.83
4		NMe ₂ ^f	408.6	718	1.21	730	288	0.82
4	SO ₂ NH ₂		122.5	681	1.19	662 ^g	295	2.01
4	NO ₂		420.3	683	1.19	679 ^h	296	1.21
4	NO ₂ ⁱ		407.5	691	1.21	679 ^h	294	1.99
8		CN	644.8	710	1.30	687	300	1.51
8	Cl		335.2	700	1.20	705	302	1.96
16	Cl	Cl	305.3	720	1.29		315	0.89
4	tetraprotonated ^j		1304.8	870	1.24	799	318	0.51

^a z-matrix input with symmetry and with all heavy atoms constrained to lie in the molecular plane except where stated otherwise; λ is the transition energy (nm) and f is the oscillator strength. ^b 1-, 8-, 15-, and 22-positions (α) and 2-, 9-, 16-, and 23-positions (β). ^c AM1 value in kcal mol⁻¹. ^d Experimental data from Table 1. ^e Data for the *meta*-^tBu derivative (In). ^f Torsion angles of the methyl carbons allowed to vary during the optimization. ^g Experimental data for the corresponding SO₂NMe₂ derivative (Ip). ^h Data for the *meta*-^tBu derivative (Ix). ⁱ Torsion angles of the oxygens allowed to vary during the optimization. ^j At the 6-, 13-, 20-, and 27-positions.

rings are able to stabilize the small electron movement to these positions in the LUMO (Figure 3). Ring substituents are predicted therefore to have only a very small effect on the B-band, in line with the experimental data (Table 1).

4. Calculations on Substituted Zinc Phthalocyanines. The structures of symmetrically substituted phthalocyanines containing four or eight substituents were calculated at the AM1 level using planar conformations for the substituents where possible, with symmetry constraints, to maximize their π -electron interactions with the macrocyclic rings. In some cases, however, these constraints caused the geometry of the macrocyclic ring to become distorted to relieve the potential clash between parts of the substituent and the lone pair of electrons at the peripheral positions of the phthalocyanine ring (see later). The structures derived from the AM1 optimization were then used directly to calculate the transition energies and oscillator strengths using a default of 64 configurations between occupied and virtual orbitals. This proved to be adequate for most derivatives, with only very small changes found in the calculated transition energies on increasing the number. However, the amino derivatives were found to be more sensitive to the number of molecular orbitals included in the CI treatment, and in these cases 100 configurations were adopted.

The introduction of four electron-donating planar trigonal NH₂ groups into the phenyl rings of the unsubstituted phthalocyanine (Ia) results in a substantial bathochromic shift (Table 5), with the greatest effect predicted at the α -positions, in line with experimental data. A similar effect is produced in the planar tetra-NHMe derivative. However, in the corresponding planar tetra- α -NMe₂ derivative, the C-NMe₂ bond is stretched to prevent clash between the hydrogen atoms of the nearest methyl groups and the lone pair of electrons at the peripheral nitrogen atoms of the macrocyclic ring. Thus, in moving from NH₂ through NHMe to NMe₂ the bond length increases from 1.368 to 1.373 to 1.389 Å. Furthermore, when the planar constraints

to the substituent geometry are removed for the tetra-NMe₂ derivative, the structure optimization produces a twisted and tetrahedral conformation at the donor nitrogens with the carbons of the two methyl groups inclined at dihedral angles of 78° and -60° to the ring plane and a resulting heat of formation which is 24.1 kcal mol⁻¹ lower than the initial planar-constrained calculation (Table 5). The reduced conjugation between the lone pair of electrons at the donor nitrogen of the NMe₂ group resulting from the twist and the change of hybridization has a dramatic effect on the calculated absorption, and the small bathochromic shift now predicted is clearly erroneous (Table 5). However, although the energy gap between the planar-constrained structure and the twisted unconstrained structure is substantial, it is nevertheless smaller than the calculated transition energy of the planar structure of 37.8 kcal mol⁻¹ (752 nm).

The constrained optimization of the corresponding β -dimethylamino derivative gives a structure which shows a smaller bathochromic shift than the α -derivative. In this case there is no potential clash with the lone pair electrons at the peripheral nitrogen atoms as the substituent is well removed from the inner macrocyclic ring. However, an alternative optimization which allows the methyl groups to move results in a structure where the methyl carbons are inclined at dihedral angles of -9.2° and -170.6°, respectively, to give an approximate tetrahedral geometry at nitrogen. This structure is only 0.1 kcal mol⁻¹ lower in energy than the fully planar conformer, and the small change in hybridization at nitrogen has only a marginal effect (-3 nm) on the transition energy (Table 5). These results suggest that the choice of planar conformations for most of the substituents discussed here is valid.

Although oxygen and sulfur donors such as SPh and OPh also produce substantial bathochromic shifts (Table 1), the corresponding alkyl derivatives were explored in the theoretical studies to simplify the calculation, particularly with respect to the z-matrix input. The presence of the OMe or OH groups at the α -position produces fairly large calculated bathochromic shifts, in line with the experimental data (Table 5). The SMe group at the α -position behaves similarly and is predicted to give a shift comparable to the OMe group.

Electron attractors such as the CN, NO₂, and Cl substituents also produce small bathochromic shifts possibly by attracting electron density from the heterocyclic ring carbons at the 5-, 7-, 12-, 14-, 19-, 21-, 26-, and 28-positions in the HOMO of zinc phthalocyanine toward the phenyl rings and so stabilize the LUMO (Figures 1 and 2). Thus, the presence of eight electron-attracting CN groups at the β -positions produces a calculated bathochromic shift of 25 nm, which is comparable to the experimental value of 15 nm (Table 1). Similarly, the presence of eight chlorine atoms at the α -positions also produces a bathochromic shift, though the magnitude is slightly less than expected.

Optimization of the α -NO₂ derivative with planar constraints results in a distortion of the phthalocyanine geometry because of a potential clash between the inner oxygen atom and the lone pair of electrons at the peripheral ring nitrogen atoms in a related way to the clash produced by one methyl group of the NMe₂ derivative discussed above. If the planar constraints to the substituted geometry are removed, the AM1 optimization produces a twisted structure, with the oxygen atoms of the NO₂ group inclined at angles of 72° and -110° to the ring plane and a heat of formation which is 12.8 kcal mol⁻¹ lower in energy than the fully planar structure (Table 5). Surprisingly, the change of geometry has little effect on the transition energy of either the Q- or B-bands, with the favored structure showing a very small bathochromic shift to match the experimental data.

In contrast, a small hypsochromic shift is calculated for four SO_2NH_2 groups at the α -positions, in line with the experimental data for the closely related SO_2NMe_2 derivative (Table 5). Here the structure optimization results in a conformation where the oxygens of the tetrahedral sulfur atom are positioned above and below the ring plane, with the nitrogen atom of the amino group in the same plane as the sulfur atom with the two hydrogens orthogonal to the ring plane on the outside edge of the molecule.

Protonation at the 6-, 13-, 20-, and 27-positions results in a very large experimental bathochromic shift, for example, of around 120 nm for the tetraprotonated copper derivative^{23,34} (see Table 1), with a similar effect expected for the zinc derivative. The calculated transition energy of the AM1-optimized tetraprotonated zinc phthalocyanine shows a very large bathochromic shift which is consistent with the experimental data (Table 5), but the magnitude is greater than expected possibly because there is no balancing counterion included in the calculation.

The effects of substituents on the position of the B-band of zinc phthalocyanine (**Ia**) are much less pronounced than the Q-band. Experimentally, the introduction of electron donors such as four α -dimethylamino groups coupled with four β -tert-butyl groups to give the octasubstituted derivative (**Ih**) results in a small hypsochromic shift relative to the unsubstituted structure. In contrast, the introduction of electron attractors such as eight cyano groups to give the octacyano derivative (**II**) produces a very small bathochromic shift, though in practice, the shifts observed in both cases may simply reflect solvent effects in moving from dimethyl sulfoxide to chlorobenzene or dimethylformamide (Table 1). The calculated results show the same trends, also in line with the arguments given earlier with the substituents producing very little effect on the B-band, though the oscillator strengths appear to vary (Table 5).

Conclusions

A combination of the AM1 and CNDOVS methods gives a reasonable account of the structures, transition energies, and oscillator strengths of zinc phthalocyanine and its derivatives. Electron donors at the phenyl ring positions facilitate the electron transition from the HOMO to the LUMO, giving rise to a large bathochromic shift in the long wavelength Q-band. In contrast, these substituents have little effect on the B-band, which is dominated by a corresponding electron transition from the HOMO-1 to the LUMO.

References and Notes

- (1) Moser, F. H.; Thomas, A. L. *Phthalocyanine Compounds*; Reinhold: New York, 1963. *Idem. The Phthalocyanines*, Vol. 1, Properties; CRC Press: Boca Raton, FL, 1983.
- (2) Leznov, C. C.; Lever, A. B. P. *Phthalocyanines: Properties and Applications*; VCH: New York, 1989.
- (3) Pariser, R.; Parr, R. G. *J. Chem. Phys.* **1953**, *21*, 466, 767. Pople, J. A. *Trans. Faraday Soc.* **1953**, *49*, 1375.
- (4) Weiss, C.; Kobayashi, H.; Gouterman, M. *J. Mol. Spectros.* **1965**, *16*, 415.
- (5) McHugh, A. J.; Gouterman, M.; Weiss, C. *Theor. Chim. Acta* **1972**, *24*, 346.
- (6) Marks, T. J.; Stojakovic, D. R. *J. Am. Chem. Soc.* **1978**, *100*, 1695.
- (7) Henrikssen, A.; Roos, B.; Sundbom, M. *Theor. Chim. Acta* **1972**, *27*, 303.
- (8) Del Bene, J.; Jaffe, H. H. *J. Chem. Phys.* **1968**, *48*, 1807, 4050; **1968**, *49*, 1221; **1968**, *50*, 1126.
- (9) Lee, L. K.; Sabelli, N. H.; LeBreton, P. R. *J. Phys. Chem.* **1982**, *86*, 3926.
- (10) Ridley, J. E.; Zerner, M. C. *Theor. Chim. Acta* **1973**, *32*, 111. Bacon, A. D.; Zerner, M. C. *Ibid.* **1979**, *53*, 21. Zerner, M. C.; Loew, G. H.; Kirchner, R. F. Mueller-Westerhoff, U. T. *J. Am. Chem. Soc.* **1980**, *102*, 589.
- (11) Nakamura, S.; Flamini, A.; Fares, V.; Adachi, M. *J. Phys. Chem.* **1992**, *96*, 8351.
- (12) Gassman, P. G.; Ghosh, A.; Ajmlof, J. *J. Am. Chem. Soc.* **1992**, *114*, 9990.
- (13) Dewar, M. J. S.; Zoebisch, E. G.; Healy, E. F.; Stewart, J. J. *Am. Chem. Soc.* **1985**, *107*, 3902.
- (14) *QCPE Program 455*, Version 6.0; Department of Chemistry, Indiana University, Bloomington, IN 47405.
- (15) Docherty, V. J.; Pugh, D.; Morley, J. O. *J. Chem. Soc., Faraday Trans. 2* **1985**, *81*, 1179. Morley, J. O.; Pugh, D. *J. Chem. Soc., Faraday Trans.* **1991**, *87*, 3021.
- (16) Francois, P.; Carles, P.; Rajzmann, M. *J. Chim. Phys.* **1977**, *74*, 606; **1977**, *76*, 328.
- (17) Nishimoto, K.; Mataga, N. *Z. Phys. Chem. (Frankfurt am Main)* **1957**, *12*, 335.
- (18) Pariser, R. *J. Chem. Phys.* **1956**, *24*, 250.
- (19) Edwards, L.; Gouterman, M. *J. Mol. Spectrosc.* **1970**, *33*, 292.
- (20) Derkacheva, V. M.; Luk'yanets, E. A. *Zh. Obshch. Kim.* **1980**, *50*, 2313; *J. Gen. Chem. USSR* **1980**, *50*, 1874.
- (21) Derkacheva, V. M.; Kaliya, O. L.; Luk'yanets, E. A. *Zh. Obshch. Kim.* **1983**, *53*, 188; *J. Gen. Chem. USSR* **1983**, *53*, 163.
- (22) Mikhaleiko, S. A.; Derkacheva, V. M.; Luk'yanets, E. A. *Zh. Obshch. Kim.* **1981**, *51*, 1650; *J. Gen. Chem. USSR* **1981**, *51*, 1405.
- (23) Wohrle, D.; Meyer, G.; Wahl, B. *Makromol. Chem.* **1980**, *181*, 2127.
- (24) Solov'eva, L. I.; Mikhaleiko, S. A.; Chernykh, E. A.; Luk'yanets, E. A. *Zh. Obshch. Kim.* **1982**, *52*, 90; *J. Gen. Chem. USSR* **1982**, *52*, 83.
- (25) Barrett, P. A.; Bradbrook, E. F.; Dent, C. E.; Linstead, R. P. *J. Chem. Soc.* **1939**, 1820.
- (26) Mikhaleiko, S. A.; Luk'yanets, E. A. *Zh. Org. Kim.* **1975**, *11*, 2216; *J. Org. Chem. USSR* **1975**, *11*, 2246.
- (27) Dewar, M. J. S.; Merz, K. M. *Organometallics* **1988**, *7*, 522.
- (28) Hunter, J. A.; Morley, J. O. *Polyhedron* **1987**, *6*, 1215.
- (29) Duggan, P. J.; Gordon, P. F. *Eur. Pat.* 155780; *Chem. Abstr.* **1987**, *105*, 70242r.
- (30) Birchall, J. M.; Haszeldene, R. N.; Morley, J. O. *J. Chem. Soc. C* **1970**, 2267.
- (31) Cambridge Structure Database, Cambridge Crystallographic Data Centre, University Chemical Laboratory, Lensfield Road, Cambridge, CB2 2EW, U.K.
- (32) Mikhaleiko, S. A.; Barkanove, S. V.; Lebedev, O. L.; Luk'yanets, E. A. *Zh. Obshch. Kim.* **1971**, *41*, 2735; *J. Gen. Chem. USSR* **1971**, *41*, 2770.
- (33) Sybyl, Version 6.0; Tripos Associates Inc.: 1699 S. Hanley Road, St. Louis, MO 63144-2913, 1992.
- (34) Gaspard, S.; Verdager, M.; Viovy, R. *J. Chem. Res., Synop.* **1979**, 271; *J. Chem. Res., Miniprint* **1979**, 3072.

JP942582A